

## BINARY RECONNECTION AND THE HEATING OF THE SOLAR CORONA

E. R. PRIEST

School of Mathematics and Statistics, University of St. Andrews, St. Andrews, Fife KY16 9SS, Scotland, UK;  
eric@mcs.st-and.ac.uk

D. W. LONGCOPE

Department of Physics, Montana State University, P.O. Box 173840, Bozeman, MT 59717-3840;  
dana@physics.montana.edu

AND

V. S. TITOV

Institut für Theoretische Physik, Ruhr-Universität Bochum, D-44780 Bochum, Germany;  
st@tp4.ruhr-uni-bochum.de

Received 2002 October 24; accepted 2003 July 29

### ABSTRACT

The relative motions of myriads of magnetic fragments in the solar surface are likely to drive magnetic reconnection and therefore heating among the magnetic field lines that spread from these fragments into the solar corona. We suggest that the fundamental mechanism is one of “binary reconnection” due to the motion of a given magnetic source relative to its nearest neighbor. The heating is due to several effects: (1) the three-dimensional reconnection of field lines that start out joining the two sources and end up joining the largest source to other more distant sources (or vice versa), so that the field line footpoints are exchanged; (2) the viscous or resistive damping of the waves that are emitted by the sources as their relative orientation rotates; and (3) the relaxation of the nonlinear force-free fields that join the two sources and that are built up by the relative motion of the sources.

*Subject headings:* MHD — plasmas — stars: coronae — Sun: corona — Sun: magnetic fields

### 1. INTRODUCTION

The surface of the Sun is covered with a multitude of magnetic sources that produce a highly complex magnetic field in the overlying corona, known as the magnetic carpet (Schrijver et al. 1998). The topological structure of this field has been considered previously by many authors (e.g., Sweet 1969; Molodenskii & Syrovatskii 1977; Gorbachev et al. 1988; Lau & Finn 1990, 1996; Inverarity & Priest 1999). The “skeletons” have been constructed of the field as a result of three (Priest, Bungey, & Titov 1997; Brown & Priest 1999) or four sources (Brown & Priest 2001; Beveridge, Priest, & Brown 2002) and by understanding the nature of the bifurcations from one topology to another as new null points or separators are created or destroyed. A skeleton (Bungey, Titov, & Priest 1996) consists of the set of null points, together with the spine curves and separatrix fan surfaces of field lines that emanate from or converge on such nulls. (The terms “spine” and “fan” were coined by Priest & Titov 1996). When two separatrices intersect, they do so in a special field line known as a “separator” that links one null point to another.

The skeleton of the field due to two unbalanced sources (*stars*) in the photosphere is shown in Figure 1, where a null point (*filled circle*) closest to the smaller source possesses a spine (*thick curve*) that joins the null point to the weaker source and to infinity. It also possesses a fan surface of field lines that arch over the weaker source in the form of a dome, which intersects the photosphere in a dashed curve (on which lies the stronger source). Part of the magnetic flux from the stronger source lies below the separatrix fan surface and links to the weaker source, while the remaining flux lies above the separatrix and links out to infinity (i.e., to distance sources).

A key question is, what is the effect of the relative motions of the photospheric sources in driving reconnection (e.g., Priest & Forbes 2000), and therefore heating, in the overlying corona? In general, this is an exceedingly complicated question as a result of the complex nature of the coronal field. So far, attention has focused on the role of “separator reconnection” at the separators that may sometimes exist in the topologies produced by three or four sources (Longcope 1996, 2001), which has been modeled numerically (Galsgaard, Parnell, & Blaizot 2000; Parnell & Galsgaard 2003).

However, the most important interaction for heating the corona may well be a more fundamental process that we consider in this paper, due to binary interactions of pairs of (unbalanced) sources, rather than due to the higher order interactions that are associated with separators. We call this process *binary reconnection*.

Several other ways in which reconnection may heat the corona after the formation of current sheets (e.g., Low 1987, 1991; Billingham, Craig, & Sneyd 1993) have been proposed. X-ray bright points are likely to be heated after flux emerges and reconnects at the boundaries of supergranules (Parnell, Priest, & Titov 1994), partly by emergence itself and partly by cancellation. However, this mechanism does not provide enough heat for the whole corona, and instead coronal loops may be heated either by separator or binary reconnection, as mentioned above, or by flux braiding, as discussed in great detail by Parker (1972, 1979, 1994) and modeled numerically by, e.g., Galsgaard & Nordlund (1996) and Gudiksen & Nordlund (2002). This approach has been further developed by Priest, Heyvaerts, & Title (2002) in their flux tube tectonics model, in which one effect of the magnetic carpet has been incorporated, namely, the way in which coronal magnetic flux is anchored in myriads of small magnetic fragments in the photosphere. As these fragments move around, current

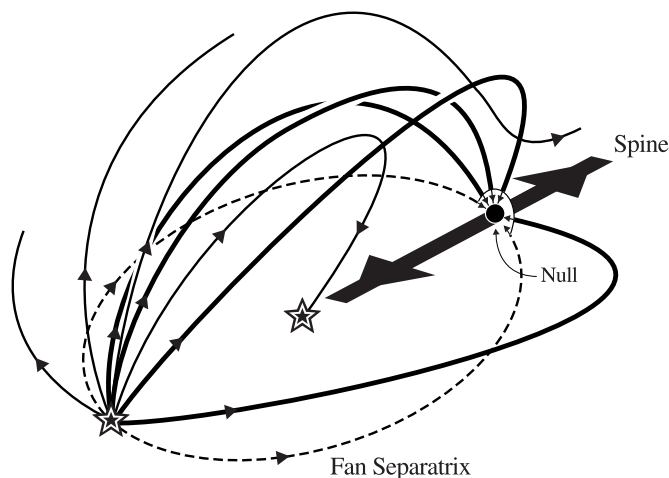


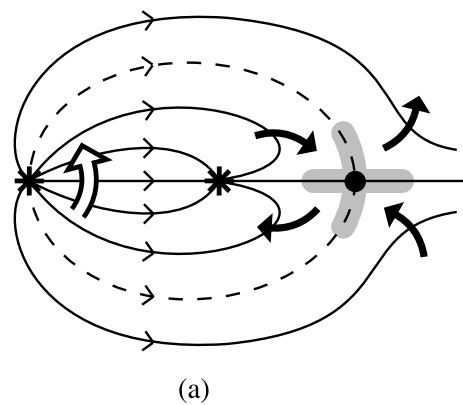
FIG. 1.—Skeleton of the field due to two unbalanced sources (*stars*)

sheets and dissipation are driven along the multitude of separatrix surfaces that separate the fluxes coming from the fragments. The present paper describes an additional process that will provide extra heating, especially low down near the solar surface, where the dominant effect at any location is likely to be due to the interaction between the two closest photospheric sources.

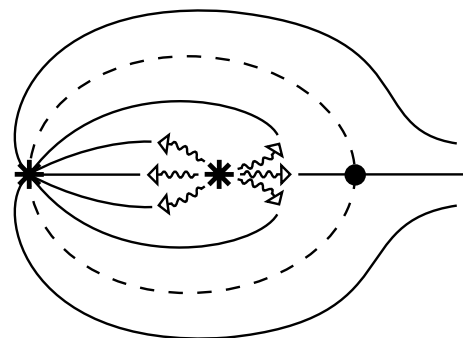
According to a well-known dimensional argument (e.g., Parker 1979), the Poynting flux through the solar surface due to horizontal motions ( $v_0$ ) on a vertical field ( $B_0$ ) and creating a horizontal field component ( $B_h$ ) is of order  $v_0 B_0 B_h / \mu$ . For typical values of the flow and field there is plenty of flux to heat the corona, but the main outstanding questions instead concern the values of  $B_h$  and of the constant of proportionality and, more importantly, the detailed manner by which reconnection, say, thermalizes this energy flux. One of the purposes of the present paper is to assess this further.

There are several contributions to the heating produced by binary reconnection (Fig. 2). The basic process (considered in § 2) is that, as two sources move around relative to one another, the magnitude of the magnetic flux joining them remains constant but the actual field lines joining one source to the other may change. In other words, particular field lines may at one time join the larger source to the smaller source, but later they may join the larger source to infinity. Thus, their connectivity has changed: magnetic reconnection has occurred.

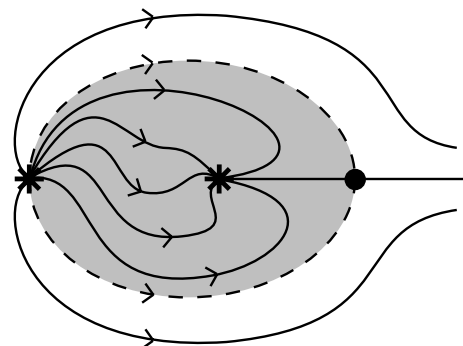
As well as the above process of laminar reconnection, which may liberate energy both at the null point and also along the separatrix surface, there are two other important energy-liberating ingredients of binary reconnection. The first (§ 3) is that the motions of the sources will generate waves that propagate outward and dissipate either viscously or ohmically. The other ingredient (§ 4) comes from the fact that general slow twisting motions or lateral relative motion of the sources will lead to a quasi-static buildup of a nonlinear force-free field within the separatrix dome, which is then likely to relax by turbulent reconnection to a linear force-free state. After describing these processes in §§ 2–4, including a comparison of time-dependent wave processes and quasi-static relaxation (§ 4.2), we conclude (§ 5) by evaluating its effectiveness for coronal heating.



(a)



(b)



(c)

FIG. 2.—Basic processes of energy release by binary reconnection: (a) laminar reconnection, (b) the dissipation of waves propagating from the sources, and (c) turbulent relaxation.

The processes of reconnection, wave propagation, and helicity injection have of course been considered before in a range of publications. What is new here, however, is the recognition that binary motions of two sources relative to one another (which may well be the most common source interaction process since it has the lowest order) can liberate heat in a variety of different ways that we describe and model. In particular, we give a qualitative description and kinematic theory for laminar binary reconnection, as well as an estimate of the free energy associated with magnetic helicity

conservation (§ 2). This is followed by a model for Alfvén wave propagation from a source (§ 3) and a theory for helicity injection and the resulting energetics of binary reconnection.

2. LAMINAR CONTRIBUTION TO BINARY RECONNECTION

We are suggesting that a key mechanism for heating the corona may be due to binary interactions of photospheric sources, rather than higher order interactions associated with separators. Thus, consider the interactions of two unbalanced sources and ask what happens as they move relative to each other: how does the field reconnect and how much heat is released? These are tough questions that we shall only be able to begin to address here.

In the frame of reference of a pair of sources, the field at the larger source may rotate and drive reconnection at the null point (Fig. 2a). Here we give first a qualitative descrip-

tion (§ 2.1) and then develop a kinematic model under the simplifying assumption that the field at large distances from the null remains potential (§ 2.2). Later, we consider the nonpotential fields that may be built up (§ 4). Throughout, we model photospheric sources of coronal flux by point sources placed on the photospheric plane, which is a standard valid procedure for calculating the magnetic field at distances larger than the source diameter and smaller than the solar radius.

2.1. Qualitative Description

Starting with the orientation of sources shown in Figure 3a where the field lines leaving the left source are spaced at  $22.5^\circ$  and those entering the right source are spaced at  $45^\circ$ , imagine one source moving relative to the other and ask what can we deduce simply from the field rotations in the cartoons of the figure. The relative motion may be split into two parts, namely, the direct approach of the sources and the rotation of one around the other. The direct

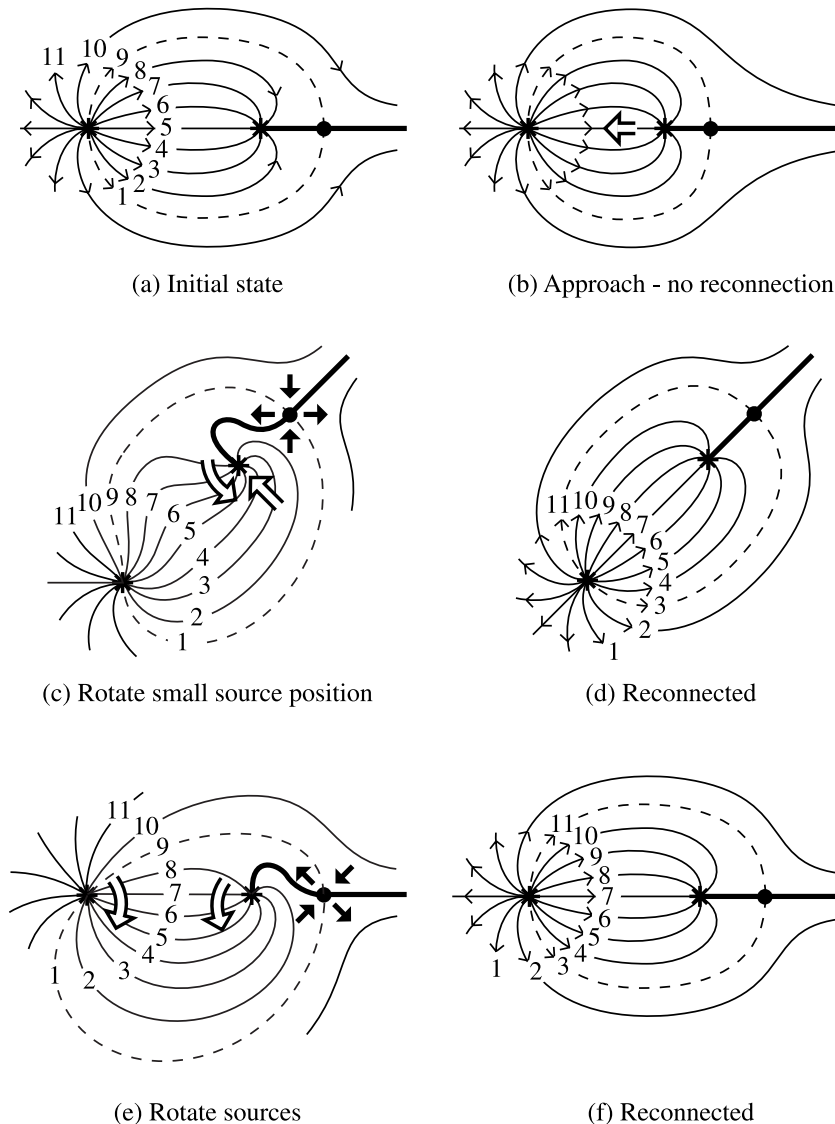


FIG. 3.—Basic laminar contribution to binary reconnection, showing a cartoon of (a) the initial state for a pair of unbalanced sources (stars) viewed from above with a null (filled circle), spine (solid line), and separatrix fan (dashed line). (b) An approach of the sources produces no reconnection, but the rotation (c) of the source position or (e) of the sources themselves drives reconnection (d and f).

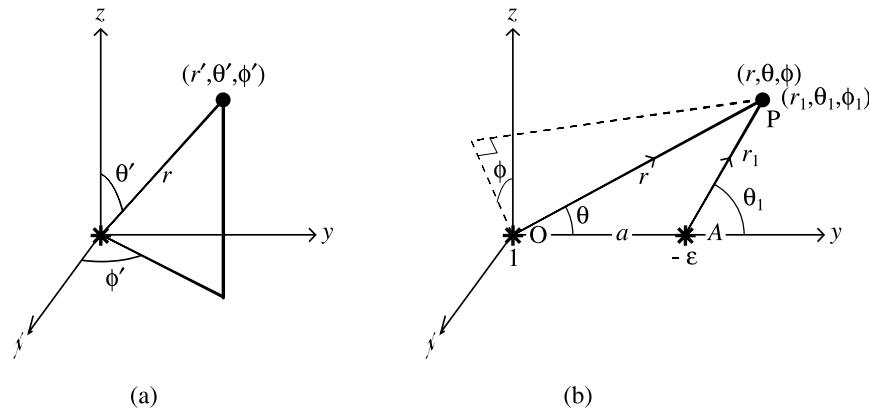


FIG. 4.—Notation for (a) a single source and (b) a pair of sources

approach (Fig. 3b) simply leads to a compression of the field lines without reconnection, whereas the rotation drives reconnection to a lower energy state. The anticlockwise rotation of the position of the smaller source around the larger by  $45^\circ$  is indicated in Figure 3c by the large straight arrow. If at the same time the small source itself rotates anticlockwise by  $135^\circ$ , as shown by the large curved arrow, then the final state (Fig. 3d) is a potential state, in which field lines 2 and 10 have reconnected, while field lines 3 and 11 have become the new separatrix field lines in the plane of the sources in place of lines 1 and 9.

Alternatively, the positions of the sources may remain fixed, while the larger source rotates by  $45^\circ$  in a clockwise sense (Fig. 3e). This again drives reconnection, and if the smaller source rotates anticlockwise through an angle of  $90^\circ$  (Fig. 3e), then the final state will be a potential field (Fig. 3f).

2.2. Kinematic Model for Laminar Element of Binary Reconnection

Let us seek to determine the nature of the electric field ( $\mathbf{E}$ ) and plasma velocity ( $\mathbf{v}$ ) outside the vicinity of the null point (where the electric currents are likely to be concentrated). In the steady state kinematic approximation for a given magnetic field,  $\mathbf{E}$  and  $\mathbf{v}$  are determined by

$$\nabla \times \mathbf{E} = 0, \tag{1}$$

which implies that

$$\mathbf{E} = -\nabla\Phi, \tag{2}$$

and by

$$\mathbf{E} + \mathbf{v} \times \mathbf{B} = 0. \tag{3}$$

Equation (3) has two implications. Taking the scalar product with  $\mathbf{B}$  and using equation (2) gives

$$\mathbf{B} \cdot \nabla\Phi = 0,$$

so that  $\Phi$  is constant along a magnetic field line. In particular, if such a field line is characterized by constant values for two functions [say,  $c(x, y, z) = \text{const}$  and  $k(x, y, z) = \text{const}$ ] that define surfaces, then

$$\Phi = \Phi(c, k). \tag{4}$$

The second consequence of equation (3) arises by taking the vector product with  $\mathbf{B}$ , namely, that the plasma velocity ( $\mathbf{v}_\perp$ ) normal to the magnetic field is

$$\mathbf{v}_\perp = \frac{\mathbf{E} \times \mathbf{B}}{B^2}. \tag{5}$$

Thus, our task is to determine the function  $\Phi(c, k)$ , and then  $\mathbf{E}$  and  $\mathbf{v}_\perp$  follow from equations (2) and (5), respectively.

2.2.1. Single Source

Consider first a point source at the origin of strength  $e$  with magnetic field

$$\mathbf{B} = \frac{e}{r^2} \hat{\mathbf{r}}$$

at a point  $(r, \theta', \phi')$  in spherical polar coordinates (Fig. 4a). Here the field lines are straight and are given by  $\theta' = \text{const}$ ,  $\phi' = \text{const}$ , and so the potential is

$$\Phi = \Phi(\theta', \phi').$$

In particular, the form

$$\Phi = -e\Omega \cos \theta' \tag{6}$$

gives an electric field

$$\mathbf{E} = -\frac{e\Omega \sin \theta'}{r} \hat{\boldsymbol{\theta}}$$

and velocity

$$\mathbf{v}_\perp = \Omega r \sin \theta' \hat{\boldsymbol{\phi}},$$

and so it corresponds to a uniform (or solid-body) rotation.

2.2.2. A Binary Pair of Sources

Suppose now that there is one source of unit strength at the origin and a smaller source of strength  $-\epsilon$  at a point A a distance  $a$  along the  $y$ -axis (Fig. 4b). The resulting magnetic field is

$$\mathbf{B} = \frac{\hat{\mathbf{r}}}{r^2} - \frac{\epsilon \hat{\mathbf{r}}_1}{r_1^2} \tag{7}$$

and contains a null at a distance

$$y_N = \frac{a}{1 - \sqrt{\epsilon}}$$

along the  $y$ -axis.

The field lines are given elegantly by constant values of

$$c = \epsilon \cos \theta_1 - \cos \theta, \quad k = \phi, \quad (8)$$

where the coordinates  $(r, \theta)$  and  $(r_1, \theta_1)$  are related by

$$r_1 \sin \theta_1 = r \sin \theta, \quad r_1 \cos \theta_1 = r \cos \theta - a,$$

so that

$$\tan \theta_1 = \frac{r \sin \theta}{r \cos \theta - a} \quad (9)$$

and

$$r_1^2 = r^2 - 2ar \cos \theta + a^2. \quad (10)$$

Furthermore, the unit vector along AP in Figure 4b is

$$\hat{r}_1 = \frac{1}{r_1} [(r - a \cos \theta) \hat{r} + a \sin \theta \hat{\theta}]. \quad (11)$$

Thus, in equation (7) the magnetic field is given in terms of  $s$  and  $\theta$  with  $\hat{r}_1$  given by equation (11) and  $r_1^2$  by equation (10), while the equation of the field lines is given by  $c = c(r, \theta)$  in equation (8) with  $\theta_1$  given by equation (9).

The question now arises, how can we choose  $\Phi = \Phi(c, \phi)$ , with  $c$  given by equation (8), in such a way that

$$\Phi \rightarrow -\Omega \cos \phi' \quad \text{as } r \rightarrow 0,$$

so as to give uniform rotation of the source at the origin? The variables  $(\theta', \phi')$  and  $(\theta, \phi)$  in Figure 4 are related by

$$\begin{aligned} \cos \theta' &= \sin \theta \cos \phi \left( = \frac{z}{r} \right), \\ \sin \theta' \sin \phi' &= \cos \theta \left( = \frac{y}{r} \right). \end{aligned} \quad (12)$$

Thus, the above question is equivalent to finding  $\Phi(c, \phi)$  such that

$$\Phi(c, \phi) \rightarrow -\Omega \sin \theta \cos \phi \quad \text{as } r \rightarrow 0,$$

where  $c = \epsilon \cos \theta_1 - \cos \theta$ .

Since  $\theta_1 \rightarrow \pi$  and so  $c \rightarrow -\epsilon - \cos \theta$  as  $r \rightarrow 0$ , the function we seek is

$$\Phi(c, \phi) = -[1 - (c + \epsilon)^2]^{1/2} \Omega \cos \phi. \quad (13)$$

On that part of the  $y$ -axis for which  $y \leq a$ , we have  $c = -\epsilon \pm 1$ , and so  $\Phi$  vanishes there. However, along the rest of the  $y$ -axis, which coincides with the spine line of the configuration,  $c = \epsilon - 1$  and hence  $\Phi = -2[\epsilon(\epsilon - 1)]^{1/2} \times \cos \phi$  to give the following  $\phi$ -component of the electric field:

$$E_\phi = -2\Omega \sqrt{\epsilon(1 - \epsilon)} \frac{\sin \phi}{R},$$

where  $R^2 = x^2 + z^2$ , which has a singularity at  $R = 0$  that is characteristic of spine reconnection (Priest & Titov 1996). Thus, the rotation of the dominant source drives spine reconnection at the null point.

### 2.2.3. "Equalized" Sources

In our steady state kinematic model, one of the consequences of equation (4) is, as we have seen, that  $\Phi$  is constant along a field line. In § 2.2.2 we have imposed a solid-body rotation of one source and so have no control over the plasma velocity at the other source. Here we explore instead the idea of "equalized" sources, where the electric potential is a sum of two potentials describing solid-body rotation for each of the sources separately. Then the motion of field lines close to the sources is a nonlinear superposition of solid-body rotation and that type of motion that was previously near the second source when the first source rotated. Because of the constancy of  $\Phi$  along a field line, one can control the motion only near one of the sources, while the other motion follows automatically. This is an inevitable restriction of steady kinematics. The reason for considering this example is then to demonstrate that for source motions different from those considered in § 2.2.2, there must be a mixture of spine and fan reconnection at the null point.

Therefore, let us here consider two sources of strengths  $q_1$  and  $-q_2$ , such that the displacement vector to an arbitrary point is inclined to the  $y$ -axis at angles  $\theta_1$  and  $\theta_2$ , respectively. The potential is then of the form

$$\Phi = \Phi(\phi, \psi),$$

where

$$\psi = q_1 \cos \theta_1 - q_2 \cos \theta_2.$$

Solid-body rotation at angular speed  $\omega_1$  for the first source would give locally

$$\Phi_1 = -\omega_1 q_1 \sin \theta_1 \cos \phi$$

and for the second source (at speed  $\omega_2$ )

$$\Phi_2 = \omega_2 q_2 \sin \theta_2 \cos \phi.$$

We superimpose these and therefore obtain a generalization of equation (13) in the form

$$\begin{aligned} \Phi = -\{ &\omega_1 [q_1^2 - (\psi - q_2)^2]^{1/2} \\ &+ \omega_2 [q_2^2 - (\psi - q_1)^2]^{1/2} \} \cos \phi. \end{aligned} \quad (14)$$

Near the first source  $\psi \approx q_1 \cos \theta_1 + q_2$ , and we find

$$\Phi \approx -\omega_1 q_1 \cos \theta'_1 + \omega_2 \cos \theta'_1 \left[ \frac{q_1(2q_2 - q_1 + q_1 \cos \theta_1)}{1 + \cos \theta_1} \right]^{1/2},$$

whereas near the second source  $\psi \approx q_1 - q_2 \cos \theta_2$ , and

$$\Phi \approx \omega_2 q_2 \cos \theta'_2 - \omega_1 \cos \theta'_2 \left[ \frac{q_2(2q_1 - q_2 - q_2 \cos \theta_2)}{1 - \cos \theta_2} \right]^{1/2}.$$

On the other hand, near the separatrix surface  $\psi = q_1 - q_2 + \delta\psi$ , and the potential becomes

$$\Phi \approx -2\omega_1 \sqrt{q_2(q_1 - q_2)} \cos \phi + \omega_2 \sqrt{2q_2 \delta\psi} \cos \phi, \quad (15)$$

where the first term arises from spine reconnection and the second from fan reconnection (Priest & Titov 1996).

### 2.3. Free Energy and Magnetic Helicity

The heating can be estimated in two ways. The first is to calculate the magnetic helicity, to relate that to the free energy (see this section), and to determine the change in self-helicity of each flux bundle as it reconnects (§ 4.2). The second way is to suppose that the twisting or relative motion of the sources launches Alfvén waves that propagate in

toward the null point and dissipate during reconnection. Thus, much of the flux that is estimated to propagate from the smaller source (§ 3) is captured within the separatrix dome and focused on the null point (e.g., Galsgaard, Priest, & Titov 2003).

To quantify the energetic role of reconnection in the quasi-static limit, where there is a slow evolution through a series of magnetic equilibria, we must deduce its effect on equilibria. All of the flux ( $F_2$ ) from the smaller source (source 2) connects to the larger, so reconnection will not change the field's connectivity. The relative motion of the sources does introduce helicity in the field. The flux domain ( $D_{12}$ ) connecting the sources will have a helicity

$$H_{12} = -\frac{\theta}{\pi} F_2^2, \quad (16)$$

since the total flux in this domain is that of the smaller source. In the case in which the larger source has spun, helicity will also have been injected onto the open field lines and will propagate outward (to infinity in the present model).

A lower bound on the field's equilibrium energy can be sought by minimizing the magnetic energy subject to a constraint on  $H_{12}$ , to give the relative helicity of the flux in domain  $D_{12}$

$$H_{12}(\alpha) = \int_{D_{12}} (\mathbf{A} + \mathbf{A}_p) \cdot (\mathbf{B} - \mathbf{B}_p) dx \quad (17)$$

(Finn & Antonsen 1985), where  $\mathbf{B}_p$  is a potential field confined to that volume occupied by  $D_{12}$  in the nonpotential field  $\mathbf{B}$ . The flux outside this domain is assumed to have a large enough volume that its helicity is irrelevant. The result of the minimization is a field that has constant  $\alpha$  inside the domain and is potential outside it:

$$\nabla \times \mathbf{B} = \begin{cases} \alpha \mathbf{B}, & x \in D_{12}, \\ 0, & \text{otherwise.} \end{cases} \quad (18)$$

There is no restriction on gauge choice for the vector potentials in equation (17). By choosing both  $\mathbf{A} = \mathbf{B}/\alpha$ ,  $\nabla \cdot \mathbf{A}_p = 0$  and  $\mathbf{A} - \mathbf{A}_p$  to be normal to the surface  $\partial D_{12}$ , it can be readily shown that

$$H_{12}(\alpha) = \frac{1}{\alpha} \int_{D_{12}} (|\mathbf{B}|^2 - |\mathbf{B}_0|^2) dx = \frac{2\mu}{\alpha} \Delta E_{12}, \quad (19)$$

where  $\Delta E_{12}$  is the free magnetic energy in domain  $D_{12}$ . The free energy ( $\Delta E_{12}$ ) is a lower bound on the free energy of the entire field. However, it is not equal to the free energy since the reference field, which is potential inside and outside  $D_{12}$ , might still have surface currents along  $\partial D_{12}$ . We use equation (19) in § 4 to deduce the heating rate.

### 3. ALFVÉN WAVE PROPAGATION FROM A SOURCE

The relative “binary” motion of pairs of sources leads to the propagation of energy from the smaller source toward the larger inside the dome (Fig. 2). The energy may dissipate either in a wavelike manner (viscously or ohmically) or quasi-statically (by the relaxation of nonlinear force-free fields), or it may do so by reconnection near the null (which can be either time dependent and wavelike or steady and quasi-static; Priest & Forbes 2000). This energy will be estimated in § 5.

Here we model the propagation of an Alfvén wave from a magnetic source in spherical polar coordinates ( $r, \theta, \phi$ ). Suppose that the background field of the source with strength  $B_e$  at distance  $L_e$  is

$$\mathbf{B}_0 = \frac{B_e L_e^2}{r^2} \hat{\mathbf{r}} \quad (20)$$

and that the wave produces a velocity ( $\mathbf{v}_1$ ) and magnetic perturbation ( $\mathbf{B}_1$ ) given by

$$\mathbf{v}_1 = v_1(r, t) \sin \theta \hat{\boldsymbol{\phi}}, \quad \mathbf{B}_1 = B_1(r, t) \sin \theta \hat{\boldsymbol{\phi}}.$$

Then the linearized ideal induction equation and low- $\beta$  equation of motion for a plasma of uniform density  $\rho_e$  are

$$\begin{aligned} \frac{\partial \mathbf{B}_1}{\partial t} &= \nabla \times (\mathbf{v}_1 \times \mathbf{B}_0), \\ \mu \rho_e \frac{\partial \mathbf{v}_1}{\partial t} &= (\nabla \times \mathbf{B}_1) \times \mathbf{B}_0, \end{aligned}$$

which reduce in our case to

$$\frac{\partial B_1}{\partial t} = \frac{1}{r} \frac{\partial}{\partial r} (r v_1 B_0), \quad (21)$$

$$\mu \rho_e \frac{\partial v_1}{\partial t} = \frac{B_0}{r} \frac{\partial}{\partial r} (r B_1). \quad (22)$$

Eliminating  $B_1$  and substituting for  $B_0$  gives a wavelike equation for  $u$ , namely,

$$\frac{\partial^2 u}{\partial t^2} = \frac{L_e^4 v_{\text{Ae}}^2}{r^4} \frac{\partial^2 u}{\partial r^2}, \quad (23)$$

where  $u = v_1/r$  and  $v_{\text{Ae}}^2 = B_e^2/(\mu \rho_e)$ . This may be solved by the WKB technique by writing

$$u = A(r) e^{i[\omega t - V(r)]},$$

so that equation (23) becomes

$$\frac{-\omega^2 r^4}{L_e^4 v_{\text{Ae}}^2} = \left( \frac{A'}{A} - iV' \right)^2 + \frac{A''}{A} - \frac{A'^2}{A^2} - iV'', \quad (24)$$

where primes denote derivatives with respect to  $r$ .

Now suppose that  $r \sim L_e$  and  $V \sim \omega L_e/v_{\text{Ae}} \ll 1$ . Then, to order  $(\omega L_e/v_{\text{Ae}})^2$ , equation (24) becomes

$$V'^2 = \frac{\omega^2 r^4}{L_e^4 v_{\text{Ae}}^2},$$

whose solution such that  $V(a) = 0$ , say (appropriate for outward propagation), is

$$V = \frac{\omega}{3L_e^2 v_{\text{Ae}}} (r^3 - a^3).$$

To next lowest order (i.e.,  $\omega L_e/v_{\text{Ae}}$ ), equation (24) implies

$$\frac{2A'V'}{A} + V'' = 0,$$

which determines the amplitude  $A(r)$  as

$$A = \frac{c}{r}$$

if  $v_1 = c$  when  $r = a$  and  $t = 0$ .

Thus, the appropriate WKB solution to equations (21) and (22) is

$$v_1 = \frac{-B_1}{\sqrt{(\mu\rho_e)}} = c \exp \left[ \frac{i\omega L_e}{v_{Ae}} \left( \frac{tv_{Ae}}{L_e} + \frac{a^3 - r^3}{3L_e^2} \right) \right], \quad (25)$$

and the resulting rate of energy propagation per unit area is the Poynting flux

$$\frac{\mathbf{E}_1 \times \mathbf{B}_1}{\mu} = \frac{-(\mathbf{v}_1 \times \mathbf{B}_0) \times \mathbf{B}_1}{\mu} = \frac{v_1 B_1 B_0 \sin^2 \theta \hat{\mathbf{r}}}{\mu},$$

which becomes, after taking the real parts of  $\mathbf{E}_1$  and  $\mathbf{B}_1$ ,

$$\frac{\mathbf{E}_1 \times \mathbf{B}_1}{\mu} = c^2 \frac{B_e L_e^2}{\mu r^2} \sin^2 \theta \cos^2 \left[ \frac{\omega L_e}{v_{Ae}} \left( \frac{tv_{Ae}}{L_e} + \frac{a^3 - r^3}{3L_e^2} \right) \right].$$

#### 4. HELICITY INJECTION AND ENERGY FLUX

In the previous section we have focused on aspects of binary reconnection that do not involve internal twisting of the closed field in the dome. However, in general, relative motions of a pair of sources are likely to build up twisted force-free structures in the field lines that join them. In this section we estimate the helicity injection that is involved (§ 4.1) and also the resulting heating when nonlinear force-free fields relax as a result of turbulent reconnection throughout the closed field below the separatrix dome (§ 4.2).

##### 4.1. Helicity Injection

In general, the rate of helicity injection when a series of flux tube sources of flux  $F_i$  move around on the solar surface is

$$\frac{dH_m}{dt} = -\frac{1}{2\pi} \left( \sum \omega_i F_i^2 + \sum_{i \neq j} \dot{\theta}_{ij} F_i F_j \right), \quad (26)$$

where  $\omega_i$  is the angular velocity of each tube and  $\theta_{ij}$  is the angle between a pair  $(i, j)$  of sources (Berger 1998). The first term represents the self-helicity of each tube, and the second is the mutual helicity between a pair of sources. Let us apply this to our two sources of flux  $F_1$  and  $F_2$ .

First of all, suppose that the sources are balanced, so that  $F_1 = -F_2$  and the field lines of both sources are rotated through the same angle  $\theta$  (Fig. 5a). Then (with  $\omega_1 = \omega_2 = \theta = \dot{\theta}_{12}$  in unit time) the change of the magnetic helicity according to equation (26) is

$$\Delta H = -\frac{1}{2\pi} (\theta F_1^2 + \theta F_2^2 + 2\theta F_1 F_2), \quad (27)$$

where the first two terms represent the self-helicity of the two tubes and the last is their mutual helicity. Since  $F_1 = -F_2$ , this vanishes, as expected (Fig. 5b).

If, on the other hand, the sources are unbalanced ( $F_1 \neq F_2$ ), the helicity injection given by equation (26) becomes

$$\Delta H = -\frac{\theta}{2\pi} (F_1 + F_2)^2.$$

The field lines joining the sources are not twisted, and so this represents the excess helicity in the open field lines coming from the dominant source, which will propagate outward.

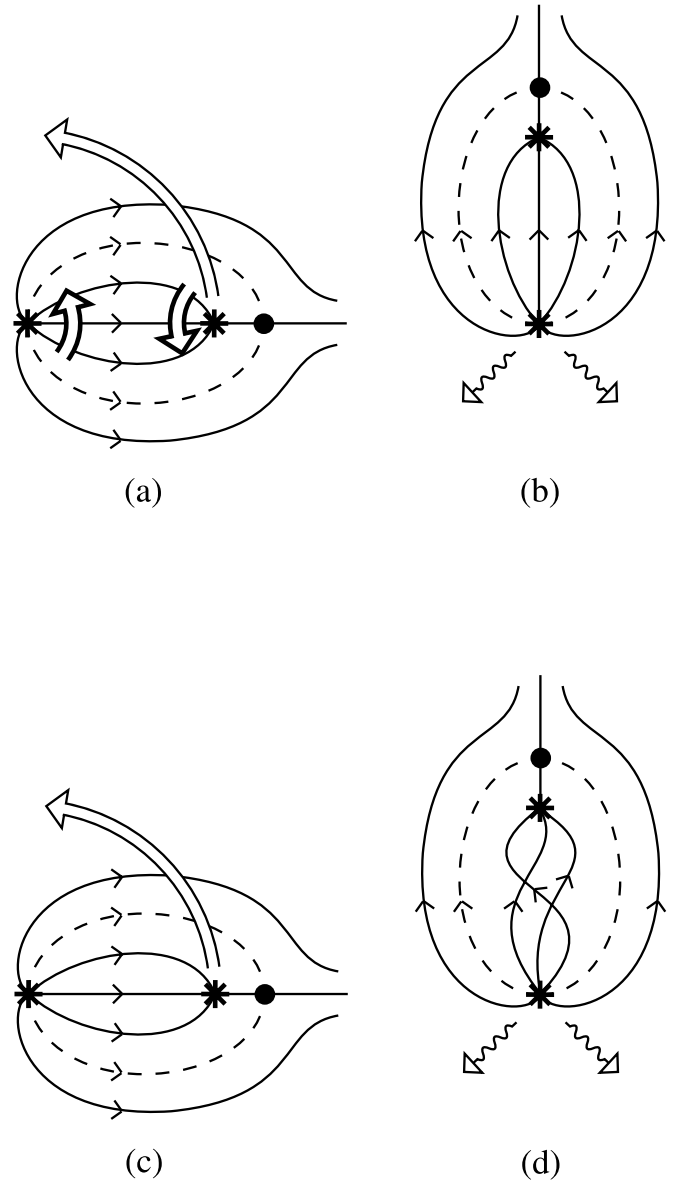


FIG. 5.—Two sources are (a) twisted and rotated by the same angle to give a state of (b) no extra magnetic helicity in the field joining the sources and twist waves on the open field lines. In (c) the sources are moved without twist, resulting in (d) a twisted flux tube and twist waves on open flux.

Next, suppose that the sources are simply moved relative to each other without any internal rotation, so that  $\omega_1 = \omega_2 = 0$ . If the angle of rotation of the relative source positions is  $\theta$ , then equation (26) implies that the increase in helicity is

$$\Delta H = \frac{1}{2\pi} 2\theta F_1 F_2. \quad (28)$$

If  $F_1 = -F_2$ , then

$$\Delta H = -\frac{\theta}{\pi} F_1^2, \quad (29)$$

and so the result is that the flux tube joining the two sources is twisted by an amount  $2\theta$ .

If, however,  $F_1 \neq -F_2$ , equation (27) can be rewritten as

$$\Delta H = \frac{\theta}{\pi} F_2^2 + \frac{\theta}{\pi} F_2 (F_1 - F_2),$$

in which the first term represents the helicity of the closed flux and the second represents the helicity that is propagated outward in a twist wave.

4.2. Energetics of Binary Reconnection

Here we calculate the energy contributed by turning a source of flux  $F$  through an angle  $\Delta\phi$  over a time  $\Delta t$  at a constant rotation rate  $\omega = \Delta\phi/\Delta t$ . Such a rotation may be a genuine rotation of a source or it may be due to the relative motion of two sources in which their relative angular position changes (cf. Longcope & Kankelborg 1999).

Suppose that the field of the source is

$$\mathbf{B}_0 = \frac{F}{2\pi r^2} \hat{\mathbf{r}}$$

and that the rotation produces an outward-propagating Alfvén wave with plasma velocity  $v_{1\phi} = r\omega \sin\theta$  and magnetic field  $B_{1\theta} = B_0 v_{1\theta}/v_{A0}$ , where  $v_{A0}$  is the local Alfvén speed. Then, as in § 3, the Poynting flux is

$$\mathbf{S} = \frac{-(\mathbf{v}_1 \times \mathbf{B}_0) \times \mathbf{B}_1}{\mu} = \frac{B_0^2}{\mu v_{A0}} v_{1\phi}^2 \hat{\mathbf{r}} = \frac{B_0^2}{\mu v_{A0}} \omega^2 \sin^2 \theta r^2 \hat{\mathbf{r}}.$$

The resulting power produced is

$$P = \int_0^{2\pi} d\phi \int_0^{\pi/2} \sin \theta r^2 S d\theta = \frac{B_0^2}{3\mu v_{A0}} r^4 \omega^2,$$

or, in terms of the flux ( $F$ ) and angle ( $\Delta\phi$ ),

$$P = \frac{F^2}{12\pi^2\mu} \frac{\omega^2}{v_{A0}} = \frac{F^2}{12\pi^2\mu} \frac{(\Delta\phi)^2}{v_{A0}(\Delta t)^2}.$$

The energy injected in time  $\Delta t$  is then

$$\Delta E = P\Delta t = \frac{F^2}{12\pi^2\mu} \frac{(\Delta\phi)^2}{v_{A0}\Delta t}, \tag{30}$$

or, in terms of the self-helicity ( $\Delta H = F^2\Delta\phi/\pi$ ) from

equation (29),

$$\Delta E = \frac{\Delta H}{12\pi\mu} \frac{\Delta\phi}{v_{A0}\Delta t}. \tag{31}$$

The way in which the released energy ( $\Delta E$ ) varies with injection time ( $\Delta t$ ) is sketched in Figure 6a. For small injection times the energy is propagated as a wave and, according to equation (31), the energy release ( $\Delta E$ ) decreases as  $(\Delta t)^{-1}$ . However, the free energy ( $\Delta E_{\text{ff}}$ ) in a linear force-free field is given from equation (19) by

$$\Delta E_{\text{ff}} = \frac{\Delta H}{2\mu} \alpha, \tag{32}$$

and this provides a minimum on the energy release. Equating equations (31) and (32) gives an expression

$$\Delta t_{\text{ff}} = \frac{\Delta\phi}{6\pi v_{A0}\alpha} \tag{33}$$

for the maximum injection time beyond which equation (31) fails and the energy conversion is quasi-static in nature.

Equating  $\Delta H$  to the helicity  $H_{\text{ff}}$  in the linear force-free field determines the value of  $\alpha$ . Changeover between a wave process and a quasi-static relaxation process occurs when wave reflections occur, namely, when

$$\Delta t = \frac{2L_{\text{eff}}}{v_{A0}},$$

where  $L_{\text{eff}}$  is the effective length of the field lines. Thus, equating this timescale to  $\Delta t_{\text{ff}}$  gives an alpha value of

$$\alpha = \frac{\Delta\phi}{12\pi L_{\text{eff}}}. \tag{34}$$

The distinction between impulsive and quasi-static heating is therefore determined by the parameter

$$\xi = \frac{v_{A0}\Delta t}{2L_{\text{eff}}}. \tag{35}$$

For impulsive energization ( $\xi < 1$ ) the energy release ( $\Delta E$ ) is given by equation (31), whereas for quasi-static energization ( $\xi > 1$ ) the energy release follows from equations (32)

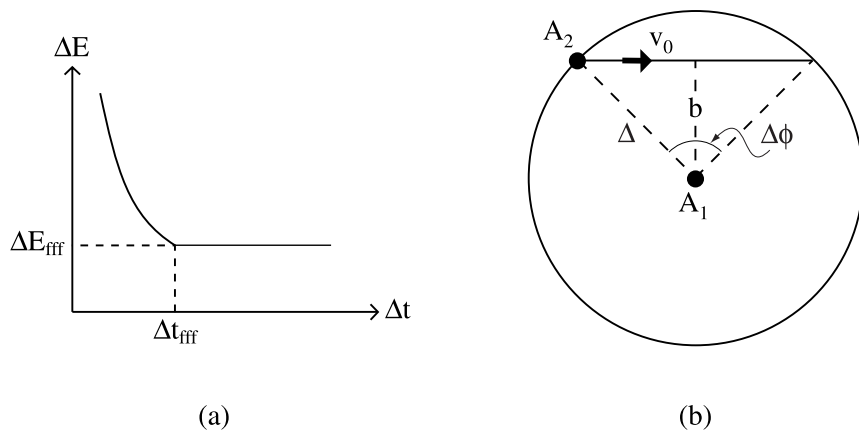


FIG. 6.—(a) Variation of the energy release ( $\Delta E$ ) as a function of the injection time ( $\Delta t$ ). For  $\Delta t > \Delta t_{\text{ff}}$  it is by quasi-static relaxation to a linear force-free field. (b) Binary collision between two magnetic sources, one at rest at  $A_1$  and the other ( $A_2$ ) originally at a distance  $\Delta$  and achieving a minimum distance of approach of  $b$ , moving at a speed  $v_0$ .

and (34) as

$$\Delta E = \frac{\Delta H}{24\pi\mu} \frac{\Delta\phi}{L_{\text{eff}}} . \quad (36)$$

Now, consider a binary collision between two sources  $A_1$  and  $A_2$  with fluxes  $F_1$  and  $F_2$ , respectively, and suppose that initially  $A_2$  is at a distance  $\Delta$  from  $A_1$ . In other words, in the frame of reference of  $A_1$ , the source  $A_2$  lies on a circle of radius  $\Delta$ . Suppose that during the collision  $A_2$  approaches within a distance  $b$  of  $A_1$  (Fig. 6b). Thus, in terms of the impact parameter ( $b$ ), the change ( $\Delta\phi$ ) in angle of orientation of  $A_1A_2$  is given by

$$\frac{\Delta\phi}{2} = \cos^{-1} \left( \frac{b}{\Delta} \right) , \quad (37)$$

while the duration ( $\Delta t$ ) of the interaction is

$$\Delta t = \frac{2\Delta}{v_0} \sin \left( \frac{\Delta\phi}{2} \right) . \quad (38)$$

The parameter  $\xi$  can then be rewritten, after identifying  $L_{\text{eff}}$  with  $b$  and substituting for  $\Delta t$  from equation (38), as

$$\xi = \frac{v_{A0}\Delta}{v_0 b} \sin \left( \frac{\Delta\phi}{2} \right) ,$$

or, after using equation (37) for  $\Delta\phi$ ,

$$\xi = \frac{v_{A0}}{v_0} \left( \frac{\Delta^2}{b^2} - 1 \right)^{1/2} . \quad (39)$$

However, the motion of magnetic sources is in practice highly sub-Alfvénic ( $v_0 \ll v_{A0}$ ), and so we deduce from equation (39) that in the vast majority of interactions (i.e., unless  $b \approx \Delta$ )  $\xi \gg 1$ , so that the interactions are quasi-static (through a series of force-free states) rather than being impulsive (mediated by wave motions).

The energy release given by equation (30) can be written in the form

$$\Delta E = \frac{F_{\text{min}}^2}{24\pi^2\mu} \frac{(\Delta\phi)^2}{L_{\text{eff}}} ,$$

where  $F_{\text{min}}$  is the smaller of the two fluxes  $F_1$  and  $F_2$  involved in an interaction. Replacing  $L_{\text{eff}}$  by  $b$  and substituting for  $\Delta\phi$  from equation (37) then gives

$$\Delta E = \frac{F_{\text{min}}^2}{6\pi^2\mu b} \left[ \cos^{-1} \left( \frac{b}{\Delta} \right) \right]^2 . \quad (40)$$

The rate of collisions ( $\nu$ ) with a source of a given sign is

$$\nu = 2\pi\Delta N_{\text{opp}} v_0 ,$$

where  $N_{\text{opp}}$  is the density of sources of opposing polarity and  $\Delta$  is the radius of a circle that contacts one source on average, so that  $\pi N_{\text{opp}} \Delta^2 = 1$ . Thus,

$$\Delta = \frac{1}{(\pi N_{\text{opp}})^{1/2}} ,$$

and the collision rate becomes

$$\nu = 2v_0 \left( \frac{N_{\text{opp}}}{\pi} \right)^{1/2} . \quad (41)$$

Using the expressions for  $\Delta E$  and  $\nu$  from equations (40) and (41) and the fact that the mean value of  $(\Delta/b)[\cos^{-1}(b/\Delta)]^2$  is about  $\sqrt{2}(\pi/4)^2 \approx 0.9 \approx 1$ , the mean rate of energy release is

$$\nu \langle \Delta E \rangle = \frac{1}{3\pi\mu} F_{\text{min}}^2 N_{\text{opp}} v_0 .$$

The heat flux ( $F_{\text{heat}}$ ) from a distribution of (majority species) sources of density  $N$  therefore becomes

$$F_{\text{heat}} = \frac{1}{3\pi\mu} F_{\text{min}}^2 N N_{\text{opp}} v_0 . \quad (42)$$

If the minority species has a fraction ( $f$ ) of the total source density ( $N_+ + N_-$ ), then  $N N_{\text{opp}} = f(1-f)$  and the heat flux becomes

$$F_{\text{heat}} = \frac{1}{3\pi\mu} F_{\text{min}}^2 f(1-f) v_0 .$$

An alternative way of writing this is in terms of the mean flux densities

$$\bar{B}_+ = \langle F_+ \rangle N_+ , \quad \bar{B}_- = \langle F_- \rangle N_- ,$$

where  $N_+$ ,  $N_-$  are the numbers of these flux elements per unit area and  $\langle F_+ \rangle$ ,  $\langle F_- \rangle$  are the mean fluxes per element. The heat flux is then

$$F_{\text{heat}} = \frac{\zeta}{3\pi\mu} \bar{B}_+ \bar{B}_- v_0 , \quad (43)$$

where  $\zeta = F_{\text{min}}/\langle F_{\text{maj}} \rangle$  is the ratio of the minority to the majority flux.

In the next section we adopt values for  $\bar{B}_+ \approx \bar{B}_-$  and  $v_0$  typical of the quiet Sun and active regions, which give a heat flux

$$F_{\text{heat}} = \frac{1}{3\pi\mu} \bar{B}_+^2 v_0 \quad (44)$$

that is enough to heat the corona provided that  $\bar{B}_+$  is large enough.

## 5. CONCLUSION

The magnetic field of the corona is rooted in the solar surface in myriads of tiny magnetic fragments, intense flux tubes of field strength  $B_t = 1200$  G and radius 100 km. The spreading with height above the photosphere of the magnetic field from these intense tubes is known as the ‘‘magnetic carpet’’ (Schrijver et al. 1998; Schrijver & Zwaan 2000) and is likely to have profound implications for the mechanisms of coronal heating. Indeed, two recent papers have started to explore some of these implications by continuing previous work of Démoulin & Priest (1997): in the first (Priest et al. 2002) a flux tube tectonics model has been proposed with heating on current sheets along the separatrices dividing the fields coming from each of the intense tube sources; in the second (Longcope & Van Ballegoijen 2002) heating along the separators where separatrices intersect is evaluated.

Here we have focused on another aspect of coronal heating, namely, the way in which the relative motion of pairs of photospheric magnetic sources drives heating in the overlying corona. There are three components to this binary

heating: (1) the reconnection of field lines whose connectivity changes as the sources move, (2) the damping of waves that are emitted by the sources, and (3) the relaxation of the nonlinear force-free fields joining the sources that are twisted up by the relative motion.

First of all, we have modeled kinematically the steady process of laminar three-dimensional reconnection as the position of one source rotates relative to the other, by calculating the resulting electric field and field line velocity. Then we have modeled the propagation of Alfvén waves away from a magnetic source as it rotates. In addition, we have evaluated the magnetic helicity injection and its relationship to the free energy. Finally, we have discussed the energetics of binary reconnection, in which quasi-static relaxation is a more effective heating mechanism than simple impulsive wave heating driven by the flyby of one source past another. Other aspects that have been given an initial treatment in a numerical model of some aspects of binary reconnection by Galsgaard & Walsh (2003) include the dynamics of the rotation of sources as the field expands and the way a perturbation focuses in on a null point.

For binary interactions between opposing sources, there is an inevitable scaling on dimensional grounds of the heat flux ( $F_{\text{heat}}$ ) with the mean flux densities ( $\bar{B}_+$  and  $\bar{B}_-$ ) of positive and negative sources and the mean relative velocity ( $v_0$ ) when two magnetic sources interact. It has the form

$$F_{\text{heat}} = \gamma \frac{\bar{B}_+ \bar{B}_- v_0}{\mu},$$

where  $\gamma$  is a dimensionless parameter. The scaling arises because each interaction between two opposite-polarity sources of flux  $F_+$  and  $F_-$ , a distance  $d$  apart, produces an energy of order  $F_+ F_- / (\mu d)$ . The energy per unit area and time is then  $F_+ F_- / (\mu d)$  times the number of interactions per unit area and time. This has the same dimensions as  $\bar{B}_+ \bar{B}_- v_0 / \mu$ , where

$$\bar{B}_+ = \langle F_+ \rangle N_+, \quad \bar{B}_- = \langle F_- \rangle N_-,$$

in terms of the mean flux ( $\langle F \rangle$ ) per element and the number ( $N$ ) of elements per unit area. According to equation (44), we have for our model deduced a value for  $\gamma$  of  $(3\pi)^{-1}$  when  $\bar{B}_+ \approx \bar{B}_-$ , so that the heat flux is

$$F_{\text{heat}} = \frac{\bar{B}_+^2 v_0}{3\pi\mu}.$$

Now, in order to compare this theoretical prediction with observations, we need well-determined values for  $F_{\text{heat}}$ ,  $\bar{B}_+$ , and  $v_0$ . The canonical values for the heating flux that are

normally quoted are  $300 \text{ W m}^{-2}$  ( $3 \times 10^5 \text{ ergs s}^{-1} \text{ cm}^{-2}$ ) for the quiet Sun and  $5000 \text{ W m}^{-2}$  ( $5 \times 10^6 \text{ ergs s}^{-1} \text{ cm}^{-2}$ ) for active regions, but these were determined by Withbroe & Noyes (1977) way back in *Skylab* days, when, for example, the temperature of active regions was thought to be only 2.5 MK. More up-to-date values that have been suggested are  $100 \text{ W m}^{-2}$  in the quiet Sun and  $10^4 \text{ W m}^{-2}$  in an active region core (Katsukawa & Tsuneta 2003). However, there is clearly a need to determine carefully the heating flux in different kinds of quiet region and in different kinds of active region and how it depends on the small-scale photospheric magnetic field. As far as the mean magnetic field is concerned, observed values range in the quiet Sun from 3 G at solar minimum to 20 G at solar maximum (Harvey 1993). Other estimates of the mean flux densities in the quiet Sun range from 1.6 (Schrijver et al. 1997) to 5 G (Welsch 2002). A reasonable value for the speed of photospheric fragments is  $0.3 \text{ km s}^{-1}$  (Hagenaar 2001).

In view of the observational uncertainties in the values of  $F_{\text{heat}}$ ,  $\bar{B}_+$ ,  $v_0$  and their variation over the solar surface and with phase in the solar cycle, it is not possible to be definite at this stage. If, however, we adopt values for  $v_0$  of  $0.3 \text{ km s}^{-1}$  and for  $\bar{B}_+ \approx \bar{B}_-$  of 20 G in the quiet Sun and 200 G in active region cores, then our theoretical rate (eq. [44]) does indeed reproduce the observed values of  $100 \text{ W m}^{-2}$  for the quiet Sun and  $10^4 \text{ W m}^{-2}$  for active regions. If the mean field is 20 G and the field of intense flux tubes with a radius of 100 km is 1200 G, then flux conservation implies that on average there is one intense flux tube that reaches the corona in each square of side 1.4 Mm in the quiet Sun. An active region mean field of 200 G, on the other hand, leads to a mean separation of intense flux tubes of only 400 km. It remains to be seen whether or not active regions, where  $\bar{B}_+ \approx \bar{B}_-$  may be less true, can be modeled as well as quiet regions by this binary reconnection process.

As well as determining better observational values in the future with, for example, the *Solar-B* and *Solar Dynamics Observatory* space missions, it will thus be of great interest to study in more detail, both theoretically and computationally, the process of coronal heating by binary connection. We conclude that binary reconnection is a promising mechanism for heating the solar corona.

Eric Priest is most grateful to the Royal Society and the EU Platon Program (HPRN-CT-2000-00153) for funding visits of Slava Titov to St. Andrews (where this idea was born) and also to colleagues and friends for making him so welcome during a summer visit to Bozeman (where most of this work was undertaken). V. S. T. gratefully acknowledges financial support also from the Volkswagen Foundation.

#### REFERENCES

- Berger, M. A. 1998, in IAU Colloq. 167, *New Perspectives on Solar Prominences*, ed. D. Webb, B. Schmieder, & D. Rust (San Francisco: ASP), 102
- Beveridge, C., Priest, E. R., & Brown, D. S. 2002, *Sol. Phys.*, 209, 333
- Billinghurst, M. N., Craig, I. J. D., & Sneyd, A. D. 1993, *A&A*, 279, 589
- Brown, D. S., & Priest, E. R. 1999, *Proc. R. Soc. London A*, 455, 3931
- . 2001, *A&A*, 367, 339
- Bungey, T. N., Titov, V. S., & Priest, E. R. 1996, *A&A*, 308, 233
- Démoulin, P., & Priest, E. R. 1997, *Sol. Phys.*, 175, 123
- Finn, J. M., & Antonsen, T. M. 1985, *Comments Plasma Phys. Controlled Fusion*, 9, 111
- Galsgaard, K., & Nordlund, A. 1996, *J. Geophys. Res.*, 101, 13445
- Galsgaard, K., Parnell, C. E., & Blaizot, J. 2000, *A&A*, 362, 395
- Galsgaard, K., Priest, E. R., & Titov, V. S. 2003, *J. Geophys. Res.*, 108, 10.1
- Galsgaard, K., & Walsh, R. W. 2003, *A&A*, submitted
- Gorbachev, V. S., Kel'ner, S. R., Somov, B. V., & Shvarts, A. S. 1988, *Soviet Astron.*, 32, 308
- Gudiksen, B. V., & Nordlund, A. 2002, *ApJ*, 572, L113
- Hagenaar, H. J. 2001, *ApJ*, 555, 448
- Harvey, K. L. 1993, Ph.D. thesis, Utrecht Univ.
- Inverarity, G. W., & Priest, E. R. 1999, *Sol. Phys.*, 186, 99
- Katsukawa, Y., & Tsuneta, S. 2003, in *COSPAR Colloq. Ser. 13, Multi-Wavelength Observations of Coronal Structure and Dynamics*, ed. P. C. M. Martens & D. Cauffman (Dordrecht: Elsevier), 61
- Lau, Y.-T., & Finn, J. M. 1990, *ApJ*, 350, 672
- . 1996, *Phys. Plasmas*, 3, 3983
- Longcope, D. W. 1996, *Sol. Phys.*, 169, 91
- . 2001, *Phys. Plasmas*, 8, 5277
- Longcope, D. W., & Kankelborg, C. C. 1999, *ApJ*, 524, 483
- Longcope, D. W., & Van Ballegoijen, A. A. 2002, *ApJ*, 578, 573
- Low, B. C. 1987, *ApJ*, 323, 358

- Low, B. C. 1991, *ApJ*, 381, 295  
Molodenskii, M. M., & Syrovatskii, S. I. 1977, *Soviet Astron.*, 21, 734  
Parker, E. N. 1972, *ApJ*, 174, 499  
———. 1979, *Cosmical Magnetic Fields* (Oxford: Clarendon)  
———. 1994, *Spontaneous Current Sheets in Magnetic Fields* (Oxford: Oxford Univ. Press)  
Parnell, C. E., & Galsgaard, K. 2003, *A&A*, submitted  
Parnell, C. E., Priest, E. R., & Titov, V. S. 1994, *Sol. Phys.*, 153, 217  
Priest, E. R., Bungey, T. N., & Titov, V. S. 1997, *Geophys. Astrophys. Fluid Dyn.*, 84, 127  
Priest, E. R., & Forbes, T. G. 2000, *Magnetic Reconnection: MHD Theory and Applications* (Cambridge: Cambridge Univ. Press)  
Priest, E. R., Heyvaerts, J., & Title, A. M. 2002, *ApJ*, 576, 533  
Priest, E. R., & Titov, V. S. 1996, *Philos. Trans. R. Soc. London*, A354, 2951  
Schrijver, C. J., Title, A. M., van Ballegoijen, A. A., Hageenaar, H. J., & Shine, R. A. 1997, *ApJ*, 487, 424  
Schrijver, C. J., & Zwaan, C. 2000, *Solar and Stellar Magnetic Activity* (Cambridge: Cambridge Univ. Press)  
Schrijver, C. J., et al. 1998, *Nature*, 394, 152  
Sweet, P. A. 1969, *ARA&A*, 7, 149  
Welsch, B. 2002, Ph.D. thesis, Montana State Univ.  
Withbroe, G. L., & Noyes, R. W. 1977, *ARA&A*, 15, 363